Intermediate-valence model for the colossal magnetoresistance in $Tl_2Mn_2O_7$

C. I. Ventura and B. Alascio
Centro Atómico Bariloche, 8400-Bariloche, Argentina
(Received 10 July 1997)

The colossal magnetoresistance exhibited by $Tl_2Mn_2O_7$ is an interesting phenomenon, as it is very similar to that found in perovskite manganese oxides, although the compound differs both in its crystalline structure and electronic properties from the manganites. At the same time, other pyrochlore compounds, though sharing the same structure with $Tl_2Mn_2O_7$, do not exhibit the strong coupling between magnetism and transport properties found in this material. Mostly due to the absence of evidence for significant doping into the Mn-O sublattice and the tendency of Tl to form conduction bands, the traditional double-exchange mechanism mentioned in connection with manganites does not seem suitable to explain the experimental results in this case. We propose a model for $Tl_2Mn_2O_7$ consisting of a lattice of intermediate-valence ions fluctuating between two magnetic configurations, representing Mn $3d$ orbitals, hybridized with a conduction band, which we associate with Tl. This model had been proposed originally for the analysis of intermediate-valence Tm compounds. With a simplified treatment of the model we obtain the electronic structure and transport properties of $Tl_2Mn_2O_7$, with good qualitative agreement with experiments. The presence of a hybridization gap in the density of states seems important to understand the reported Hall data. [S0163-1829(97)05345-9]

I. INTRODUCTION

Perovskite manganese oxides like $La_{1-x}M_xMnO_3$ (M=Ca,Sr,Ba) have been the subject of study for many years,[1] and a strong correlation between transport properties and magnetism was recognized. Shortly after the discovery of these materials, the double-exchange mechanism was proposed[2] to describe the interactions between the Mn ions. Due to the divalent substitution for La^{3+}, itinerant e_g holes are doped into the antiferromagnetic insulating parent compound $LaMnO_3$, and Mn ions appear in a mixed-valence state. Double exchange occurs between heterovalent Mn pairs (Mn^{3+}-Mn^{4+}) by simultaneous transfer of an electron from Mn^{3+} to O^{2-} and O^{2-} to Mn^{4+}. As this transfer occurs, necessarily conserving the spin orientation, an effective ferromagnetic coupling appears due to the intra-atomic Hund's rule requirement.[2] Clearly, in this framework the carrier hopping is intrinsically coupled to and enhanced by the mutual alignment of the two magnetic moments. As a result, resistivity will depend on the spin disorder and is expected to display pronounced features at the ferromagnetic ordering transition temperature (T_c). Application of a magnetic field, which favors alignment of the local spins, will produce a decrease of the resistivity.

Interest in the study of perovskite manganese oxides was renewed recently, as colossal magnetoresistance (CMR) was observed near the ferromagnetic ordering temperature.[3] At present, there is strong debate as to whether the double-exchange mechanism and theoretical models based solely on it are able to account quantitatively for the observed transport and magnetic properties of the manganese perovskites. It has been proposed that other ingredients such as disorder,[4] Jahn Teller distorsions,[5] charge ordering,[6] etc., could play an important role and should be taken into account.

In 1996 colossal magnetoresistance was reported for the nonperovskite $Tl_2Mn_2O_7$ compound.[7–9] The material undergoes a ferromagnetic transition with $T_c \sim 140$ K.[7–10] Below the ordering temperature, the compound is ferromagnetic and metallic, whereas above T_c it is paramagnetic. The magnetoresistance maximum around the ferromagnetic ordering temperature is similar to that obtained for the manganese perovskites. The sharp decrease in resistivity with the development of spontaneous magnetization below T_c and the magnetoresistance with field-induced magnetization above T_c indicate a strong coupling between transport and magnetism in $Tl_2Mn_2O_7$, similar to that in perovskite manganese oxides.[7–10] Nevertheless, important differences arise regarding crystalline structure and electronic properties. In fact $Tl_2Mn_2O_7$ is characterized by a ''pyrochlore'' $A_2B_2O_7$ structure,[11] consisting of strongly distorted AO_8 cubes and slightly distorted BO_6 octahedra. Each metal atom (A or B) forms a three-dimensional network of corner-sharing tetrahedra.[12] The interpenetrating sublattices in $Tl_2Mn_2O_7$ are, respectively, given by Tl_2O and Mn_2O_6.[7,9,13] The tetrahedral Mn_2O_6 network differentiates the pyrochlores from the perovskite ABO_3 structure, with a cubic MnO_6 network. There are also significant differences in the bond length and angle between Mn and O in the MnO_6 octahedra, which in $Tl_2Mn_2O_7$ are both smaller than for CMR perovskites[9,10,7] as well as almost temperature independent, thereby indicating negligible correlations between spin and lattice.[10] Considering electronic properties, an important difference with the hole-doped perovskites comes from Hall experiment data,[7] indicating a very small number of electronlike carriers: $\sim 0.001-0.005$ conduction electrons per formula unit. The authors of Refs. 7 and 9 mention that such Hall data could result from a small number of carriers in the Tl $6s$ band. Assuming $Tl^{3+}_{2-x}Tl^{2+}_xMn^{4+}_{2-x}Mn^{5+}_xO_7$ with $x \sim 0.005$ the data could be accounted for.[9] This would seem to indicate a very small doping into the Mn^{4+} state,[7,9] in contrast to manganese perovskites where CMR is obtained around 30% of hole doping. It is important to take notice also of the different origin of the doping. Recent electronic structure calculations for

$Tl_2Mn_2O_7$ (Ref. 13) indicate that the bands inmediately below the Fermi level correspond mainly to Mn t_{2g} states, above the Fermi level appear Tl $6s$ bands, while O states are mixed with these around the Fermi level. Another calculation by Singh[14] obtains a strong spin differentiation in the electronic structure around the Fermi level in the ferromagnetic ground state. The majority spin Mn-t_{2g}–O-$2p$ bands below the Fermi level are separated by a gap from the Mn-e_g-derived bands, though there is also a mixing with Tl and O states above and below the Fermi level. Thus a small near-band-edge Fermi surface is obtained. For the minority channel instead, a highly dispersive band with a strong admixture of Mn, Tl, and O is found around the Fermi level, leading to a metallic minority spin channel.[14]

Mostly due to the absence of evidence for significant doping in the pyrochlore Mn-O sublattice and due to the tendency of Tl to form $6s$ conduction bands (unlike in manganese perovskites where the rare-earth levels donate charge to the Mn-O bands but are otherwise electronically inactive), among other differences between the compounds discussed above, it has been speculated that a double-exchange mechanism similar to that of perovskites is unlikely to be effective in $Tl_2Mn_2O_7$,[7–10,13,14] accounting for the experimental results. Based on all these facts, we decided to explore the suitability of a different model, to provide an explanation for CMR in pyrochlore $Tl_2Mn_2O_7$. It may be useful to remark here that related pyrochlore compounds have been the subject of experimental study, and while some (A=Y, Lu) revealed no long-range magnetic order,[12] $In_2Mn_2O_7$ exhibits a similar ferromagnetic transition but the ordered phase remains insulating.[8,10] In this sense, the behavior of $Tl_2Mn_2O_7$ is very interesting due to its unique characteristics and striking differences with other known pyrochlores and CMR compounds.

In the following section we will describe the model we employed for the calculation of the electronic structure and transport properties of $Tl_2Mn_2O_7$. The intermediate-valence (IV) model was proposed originally for the study of Tm compounds.[15,16] Basically, a periodic array of mixed valent ions, fluctuating between two magnetic configurations, would represent the Mn ions appearing in $Tl^{3+}_{2-x}Tl^{2+}_{x}Mn^{4+}_{2-x}Mn^{5+}_{x}O_7$. These would be responsible for magnetism. A conduction band would represent the Tl $6s$ orbitals, which hybridize with the IV ions. For simplicity, we do not take into account the O orbitals. Through hybridization a gap can appear in the density of states. Transport is due to carriers in the conduction bands. The scattering mechanism originating from the hybridization with the IV lattice is dependent on the magnetic configuration of the lattice or spin disorder in the material. As a result, electric conduction and magnetism are intrinsically coupled and CMR results on application of a magnetic field. In Sec. III we will make a complete presentation and discussion of the results obtained with our treatment of the model. A short presentation of our approach to the problem with some preliminary results has been given before.[17] In Sec. IV a summary of our study of $Tl_2Mn_2O_7$ is given.

II. MODEL AND ANALYTICAL METHOD

The model to be introduced in this section was proposed originally for the description of intermediate-valence Tm compounds.[15,16] These compounds distinguish themselves from other IV rare earths by evidencing a rare sensitivity to the application of magnetic fields in many physical properties, like resistivity, specific heat, thermal expansion, etc. The exactly solvable impurity model which incorporates the most important feature for TmSe, namely, valence fluctuations between two magnetic configurations (corresponding to Tm^{2+}:$4f^{12}$ and Tm^{3+}:$4f^{13}$), was shown[15] to describe most of the peculiar features of the magnetic properties of paramagnetic intermediate valence Tm compounds. The impurity model resistivity exhibits an explicit quadratic dependence with the magnetization.[15] Such behavior has also been found in transport experiments slightly above T_c for colossal MR pyrochlores[7] and manganese perovskites.[18] Employing the periodic version of the model[16] the phase diagram at $T=0$ was obtained, indicating magnetic ordering. A ferromagnetic metallic phase appears for nonstoichiometric samples, while an antiferromagnetic insulating ground state is obtained for stoichiometric ones. Calculations of the specific heat and magnetic susceptibility in the paramagnetic phase treated with the coherent potential approximation[19] (CPA) were done and the neutron-scattering spectrum was studied.[16] Many of these results are reminiscent of the behavior of $Tl_2Mn_2O_7$ and other CMR compounds discussed in the previous section. In fact, for manganese perovskites a similar model has been considered[20] to propose the possibility of a metal-insulator transition.

We will now present the model proposed for $Tl_2Mn_2O_7$, considering that experimental results[9] would be compatible with the presence of mixed-valent Mn^{4+}/Mn^{5+} in the form $Tl^{3+}_{2-x}Tl^{2+}_{x}Mn^{4+}_{2-x}Mn^{5+}_{x}O_7$, as discussed in the previous section. The model[16] describes a periodic lattice of intermediate-valence ions, which fluctuate between two magnetic configurations. To simplify the problem, these are associated with single ($S=1/2$) or double occupation ($S=1$) of the ion. It is assumed that the results are dependent on the availability of two magnetic configurations and not by their detailed structure.[15] The IV ions are hybridized to a band of conduction states. The Hamiltonian considered is[16]

$$H=H_L+H_c+H_H, \tag{1}$$

where

$$H_L=\sum_j \left(E_\uparrow|j\uparrow\rangle\langle j\uparrow|+E_\downarrow|j\downarrow\rangle\langle j\downarrow|\right)$$
$$+\left(E_+|j+\rangle\langle j+|+E_-|j-\rangle\langle j-|\right),$$

$$H_c=\sum_{k,\sigma}\epsilon_{k,\sigma}c^\dagger_{k,\sigma}c_{k,\sigma},$$

$$H_H=\sum_{i,j} V_{i,j}(|j+\rangle\langle j\uparrow|c_{i,\uparrow}+|j-\rangle\langle j\downarrow|c_{i,\downarrow})+\text{H.c.}$$

H_L describes the lattice of IV ions, which for $Tl_2Mn_2O_7$ we would identify with the Mn ions. The $S=1/2$ magnetic configuration at site j is represented by states $|j\sigma\rangle$ ($\sigma=\uparrow,\downarrow$) with energies E_σ, split in the presence of a magnetic field B according to

$$E_{\uparrow(\downarrow)}=E-(+)\mu_0 B. \tag{2}$$

The $S=1$ magnetic configuration is considered in the highly anisotropic limit, where the $S_z=0$ state is projected out of the subspace of interest as in Refs. 15 and 16. This has been done for the sake of simplicity, as will be discussed shortly. The $S=1$ states at site j are then represented by $|js\rangle (s=+,-)$ and energies E_s, split by the magnetic field as

$$E_{\pm}=E+\Delta \mp \mu_1 B. \tag{3}$$

H_c describes the conduction band, which for $Tl_2Mn_2O_7$ we would identify with the Tl $6s$ conduction band.

The hybridization term H_H describes valence fluctuations between the two magnetic configurations at one site, mediated by the conduction electrons. For example, promoting a spin-up electron into the conduction band the IV ion at site j can pass from state $|j+\rangle$ to state $|j\uparrow\rangle$. Notice that the highly anisotropic limit considered inhibits any spin-flip scattering processes, which would involve transitions between the excluded $S_z=0$ state of the $S=1$ configuration and the $S=1/2$ states mediated by conduction electrons of opposite spin. So the direction of the local spin at each site is conserved, and IV ions only hybridize with conduction electrons of parallel spin. This will allow for an important simplification in the solution of the scattering problem, by separating it in two parts associated with the spin orientation of the conduction electrons.

The Hamiltonian can be rewritten in terms of the following creation (and the related annihilation) operators for the local orbitals[16] (Mn $3d$ orbitals, in this case):

$$d^{\dagger}_{j,\uparrow}=|j+\rangle\langle j\uparrow|,$$

$$d^{\dagger}_{j,\downarrow}=|j-\rangle\langle j\downarrow|, \tag{4}$$

for which one has

$$[d_{i,\uparrow},d^{\dagger}_{j,\uparrow}]_+=\delta_{i,j}(P_{i,\uparrow}+P_{i,+}),$$

$$[d_{i,\downarrow},d^{\dagger}_{j,\downarrow}]_+=\delta_{i,j}(P_{i,\downarrow}+P_{i,-}),$$

$$P_{i,+}+P_{i,\uparrow}+P_{i,-}+P_{i,\downarrow}=1,$$

where $P_{j,\alpha}=|j\alpha\rangle\langle j\alpha|$ are projection operators onto the local magnetic configuration states. The local hamiltonian now reads

$$H_L=(\Delta-\mu_D B)\sum_j d^{\dagger}_{j,\uparrow}d_{j,\uparrow}+(\Delta+\mu_D B)\sum_j d^{\dagger}_{j,\downarrow}d_{j,\downarrow},$$

$$\mu_D=\mu_1-\mu_0. \tag{5}$$

Now advantage will be taken of the type of hybridization present, resulting from the highly anisotropic limit chosen for the $S=1$ states. Given a certain configuration for the occupation of the local orbitals at all sites by spin-up or -down electrons, the spin-up conduction electrons will hybridize only with those IV ions occupied by spin-up electrons (i.e., in $\uparrow$ or $+$ local states). One can simulate this by including a very high local correlation energy ($U\to\infty$) to be paid in the event of mixing the conduction electron with ions occupied by opposite-spin electrons. Concretely, we take[16]

$$H=H_{\uparrow}+H_{\downarrow},$$

$$H_{\uparrow}=(\Delta-\mu_D B)\sum_{j\in\uparrow} d^{\dagger}_{j,\uparrow}d_{j,\uparrow}+U\sum_{j\in\downarrow} d^{\dagger}_{j,\uparrow}d_{j,\uparrow}$$

$$+\sum_k \epsilon_{k,\uparrow}c^{\dagger}_{k,\uparrow}c_{k,\uparrow}+\sum_{i,j}(V_{i,j}d^{\dagger}_{j,\uparrow}c_{i,\uparrow}+\text{H.c.}). \tag{6}$$

$H_{\downarrow}$ is analogous to $H_{\uparrow}$, one having only to reverse the sign of the magnetic field and the spin orientation. In the following, we neglect the splitting of the conduction-band energies in the presence of the magnetic field B ($\epsilon_{k,\sigma}\equiv\epsilon_k$) and take for the hybridization $V_{i,j}=V\delta_{i,j}$.

Given a certain configuration of spin orientations distributed among the sites, one can now solve two separate problems described by $H_{\uparrow}$ and $H_{\downarrow}$, respectively. Each corresponds to the problem of a band of conduction electrons of a given spin orientation, hybridized with a binary alloy characterized by the spin orientation of the electrons occupying the local orbitals. These problems we solve with a generalization of the CPA approximation, as in Ref. 16. A similar treatment was used by Sakai *et al.*[21] We introduce an effective diagonal self-energy for the local orbitals, $\Sigma_{(d)\sigma}(\omega)$, for the H_{σ} alloy problem, through which on average translational symmetry is restored. We will now sketch the solution of the spin-up problem, the extension to the spin-down case being straightforward.[16]

For spin up, the effective Hamiltonian reads

$$H_{\text{eff},\uparrow}(\omega)=[\Delta-\mu_D B+\Sigma_{(d)\uparrow}(\omega)]\sum_j d^{\dagger}_{j,\uparrow}d_{j,\uparrow}$$

$$+\sum_k \epsilon_k c^{\dagger}_{k,\uparrow}c_{k,\uparrow}+\sum_j (Vd^{\dagger}_{j,\uparrow}c_{j,\uparrow}+\text{H.c.}).$$

In terms of the effective Hamiltonian, the effective propagator in Fourier space can be calculated (a 2×2 matrix here, with components associated with the c and d spin-up bands):

$$G^k_{\text{eff},\uparrow}(\omega)=\frac{1}{\omega-H^k_{\text{eff},\uparrow}(\omega)}. \tag{7}$$

In the CPA the effective propagator is taken equal to the ensemble average of the propagator determined by $H_{\uparrow}$. The average local Green's functions obtained can be expressed as

$$\langle\langle c_{j,\uparrow},c^{\dagger}_{j,\uparrow}\rangle\rangle(\omega)=\frac{1}{N}\sum_k \frac{1}{\omega-\epsilon_k-V^2/[\omega-\sigma_{(d)\uparrow}(\omega)]},$$

$$\langle\langle d_{j,\uparrow},d^{\dagger}_{j,\uparrow}\rangle\rangle(\omega)=\frac{1}{\omega-\sigma_{(d)\uparrow}(\omega)}+\frac{V^2}{[\omega-\sigma_{(d)\uparrow}(\omega)]^2}\langle\langle c_{j,\uparrow},c^{\dagger}_{j,\uparrow}\rangle\rangle(\omega), \tag{8}$$

where

$$\sigma_{(d)\uparrow}(\omega)=\Delta-\mu_D B+\Sigma_{(d)\uparrow}(\omega). \tag{9}$$

The CPA equations obtained to determine self-consistently the effective spin-up and -down self-energies relate them directly to the local Green's functions for the IV ions:[16]

$$\Sigma_{(d)\uparrow}(\omega)=\frac{p-1}{\langle\langle d_{j,\uparrow},d_{j,\uparrow}^{\dagger}\rangle\rangle(\omega)},$$

$$\Sigma_{(d)\downarrow}(\omega)=\frac{-p}{\langle\langle d_{j,\downarrow},d_{j,\downarrow}^{\dagger}\rangle\rangle(\omega)}. \tag{10}$$

Here p denotes the concentration of spin-up sites, including single and double occupation of the ion by spin-up electrons: $p=\langle P_{i,\uparrow}+P_{i,+}\rangle$. Due to the correlations included, for the densities of states the following hold:

$$\int_{-\infty}^{\infty}d\omega\rho_{c,\sigma}(\omega)=1,$$

$$\int_{-\infty}^{\infty}d\omega\rho_{d,\uparrow}(\omega)=p,\quad \int_{-\infty}^{\infty}d\omega\rho_{d,\downarrow}(\omega)=1-p. \tag{11}$$

Given a concentration p, which is determined by the magnetization, we solve the CPA equations (spin up and down) self-consistently together with the total number of particles equation, through which the chemical potential is determined.

To take into account the effect of temperature on the magnetization in a simple form and describe qualitatively the experimental data in pyrochlores,[7,9,10] we used a simple Weiss molecular field approximation to obtain the magnetization at each temperature. A similar approach was adopted before for calculations of the magnetoresistivity in Ce compounds.[22] For a ferromagnet with critical temperature T_c, saturation magnetization $M_{\rm sat}$, and local magnetic moments of magnitude μ which can align with an external magnetic field B one has

$$\frac{M}{M_{\rm sat}}=\tanh\left(\frac{\mu B}{k_BT}+\frac{T_cM}{TM_{\rm sat}}\right). \tag{12}$$

Concerning the application of this approximation for the magnetization to our model for $Tl_2Mn_2O_7$ we take the local magnetic moment μ coincident with the experimental value for $M_{\rm sat}$, roughly $3\mu_B$ per Mn ion.[10] This is an intermediate value between the local moments for Mn^{5+}, of $3.87\mu_B$, and Mn^{4+}, of $2.83\mu_B$.

Once obtained the magnetization from Eq. (12), we determine the concentration p of ions occupied by spin-up electrons using the relation between them

$$M=[p-(1-p)]\mu. \tag{13}$$

This simple equation expresses the intrinsic link between the magnetic order measured by the magnetization and the transport properties which are determined by the CPA self-energies obtained solving the alloy problems corresponding to a concentration p of spin-up sites in the sample, as will be shown next.

We now consider the determination of transport properties. Using the Kubo formula it has been proved before[23] that no vertex corrections to the electrical conductivity are obtained in CPA for a one-band model with diagonal disorder, due to the short range of the atomic scattering potentials. For the same reason, mainly, no vertex corrections to the conductivity were obtained by Brouers *et al.*[24] with a CPA treatment of an s-d model for disordered noble- and transition-metal alloys. Their analysis also applies to our problem. Furthermore, in the absence of a direct hopping term between local orbitals only the conduction band will contribute to the conductivity in our case.[24]

As in Refs. 23, 24, and 21 we can obtain the conductivity through Boltzmann equation in the relaxation time approximation as

$$\sigma=\sigma_{c,\uparrow}+\sigma_{c,\downarrow},$$

$$\sigma_{c,\uparrow}=n_ce^2\int d\omega\left(-\frac{\partial f(\omega)}{\partial\omega}\right)\tau_{c,\uparrow}^{k}(\omega)\Phi(\omega), \tag{14}$$

where f is the Fermi distribution, n_c the total number of carriers per unit volume, and the relaxation time for spin-up conduction electrons is

$$\tau_{c,\uparrow}^{k}(\omega)=\frac{\hbar}{2|\mathrm{Im}\Sigma_{c\uparrow}^{k}(\omega)|}. \tag{15}$$

From Eq. (8) the self-energy for conduction electrons is related to the effective medium CPA self-energy through

$$\Sigma_{c\uparrow}^{k}(\omega)=\frac{V^2}{\omega-\sigma_{(d)\uparrow}(\omega)}, \tag{16}$$

and is actually k independent. $\Phi=(1/N)\,\Sigma_k v_c^2(\epsilon_k)\,\delta(\omega-\epsilon_k)$, where $v_c(\epsilon_k)$ is the conduction electron velocity. The extension of these formulas for spin down is straightforward.

Considering temperatures much lower than the Fermi temperature, one can approximate $\Phi(\omega)\sim v_F^2\rho_c^{(0)}(\omega)$, v_F being the Fermi velocity. The results presented here were obtained assuming for simplicity a semielliptic density of states for the bare conduction band $\rho_c^0(\omega)$. In this case, as can be seen from Eq. (8), the local Green's function for conduction electrons also will have a semielliptic form [with the energies shifted by $\Sigma_{c\sigma}^{k}(\omega)$].

III. RESULTS AND DISCUSSION

We now present the results obtained for this model with the parameters $W=6$ eV for the semielliptic bare conduction half-bandwidth (centering the conduction band at the origin), $E=0$, $\Delta=-4.8$ eV, and $V=0.6$ eV. To reproduce qualitatively the experimental magnetization data[7,9,10] we take T_c as 142 K and a saturation value for the magnetization of $3\mu_B$ per Mn ion (like that of free Mn^{4+} ions) in the Weiss molecular-field approximation, as well as $\mu_D=1\mu_B$. In Fig. 1 we plot the temperature dependence of the magnetization obtained for different values of the magnetic field.

In Fig. 2(a) we show the hybridization gap obtained in the CPA spin-up densities of states at $T=0$ with those parameters. No gap occurs in the spin-down c density of states, as there is strictly no spin-down d density of states to hybridize with in the ordered state ($p=1$), due to the sum rule of Eq. (11). In Fig. 2(b) we observe that at temperatures above T_c there still are hybridization gaps present for spin-up bands,

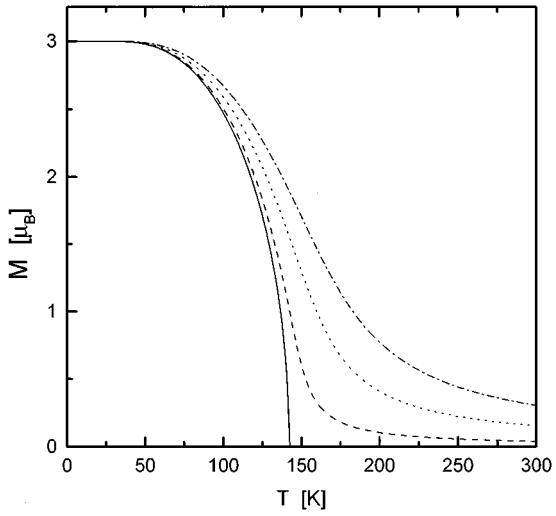

FIG. 1. Magnetization as a function of temperature for magnetic fields: $B=0$ (solid line), 1 T (dashed line), 4 T (dotted line), and 8 T (dot-dashed line). Parameters: $T_c=142$ K; $M_{\rm sat}=3\,\mu_B$, and $\mu_D=1\mu_B$.

and similar gaps have been opened for the spin-down c and d bands (or at least pseudogaps, as is the case for spin-down bands at the higher magnetic fields considered: $B=4$ and 8 T).

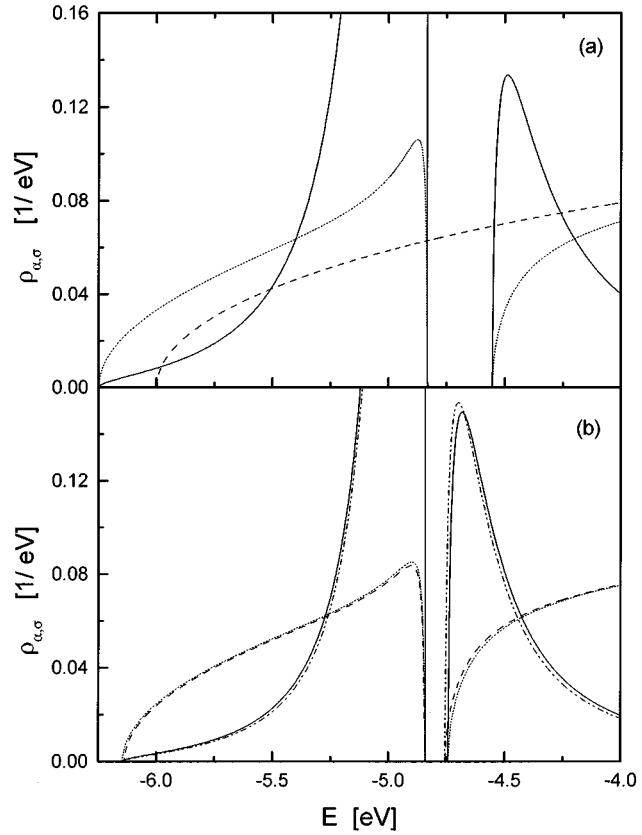

FIG. 2. Local densities of states as a function of energy at $B=1$ T and (a) $T=0$, (b) $T=200$ K. $\rho_{c,\uparrow}$ (dotted line), $\rho_{c,\downarrow}$ (dashed line), $\rho_{d,\uparrow}$ (solid line), and $\rho_{d,\downarrow}$ (dot-dashed line). Parameters: $W=6$ eV, $E=0$, $\Delta=-4.8$ eV, $V=0.6$ eV, and others as in Fig. 1.

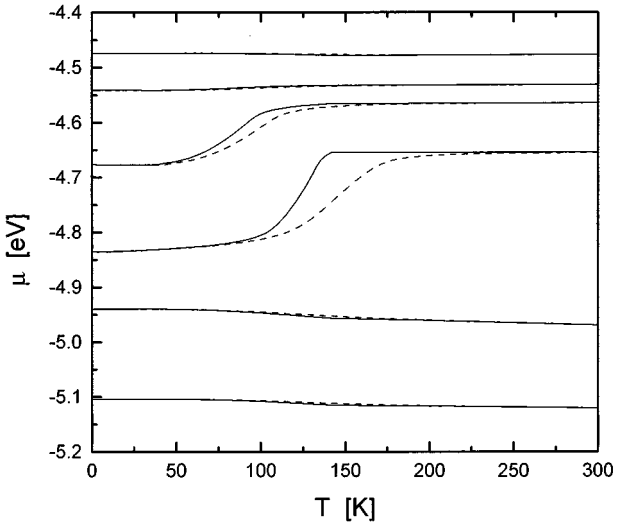

FIG. 3. Chemical potential as a function of temperature. For various fillings, from top to bottom: $n=1.085$, 1.07, 1.06, 1.03, 0.3, and 0.15. Solid lines, $B=0$; dashed lines, $B=8$ T. Parameters as in Fig. 2.

The temperature dependence of the chemical potential is plotted in Fig. 3 for various values of the total number of particles: below, through, and above the hybridization gap. Notice that the chemical potential is only sensible to the magnetic field when it falls inside the gap, outside which the temperature dependence is also very smooth.

In Fig. 4(a) we show the resistivity curves obtained for three different values of filling, in the absence of a magnetic field. The results can be qualitatively understood in the following way. At $T=0$ the resistivity is zero due to the absence of spin disorder, hence of scattering as can be seen quickly from Eqs. (10), (15), (16), and (9) with $p=1$. At finite temperatures the ''impurity approximation''[15] is useful to explain the results obtained: A given spin component of resistivity is proportional to the conduction-electron relaxation time for that spin direction at the Fermi level, which in turn is proportional to the d density of states of that spin direction at the same energy. At zero temperature there is no spin-down resistivity due to the absence of a spin-down d density of states, as obtained from Eq. (11). As the temperature increases, spin disorder appears and the d-down density of states becomes finite, and hence resistivity increases. At T_c paramagnetism sets in, and the d densities of states for both spins tend to become equal; hence the total resistivity takes a value about half of theirs. The small negative slope of resistivity at $B=0$ above T_c can be adscribed to the decrease of the d density of states at the Fermi level with temperature. The absolute values of resistivity depending on filling are distributed corresponding to the respective values of the d density of states at the Fermi level. In cases when the Fermi level falls inside the hybridization gap our resistivity results seem not very reliable, in accordance with the limitations of validity of the Boltzmann treatment for transport.[25]

In Fig. 4(b) we depict the resistivity curves obtained for different magnetic fields at a filling corresponding to having placed the Fermi level slightly above the gap, $n=1.085$. This is the situation of interest in order to explain the transport properties of $Tl_2Mn_2O_7$, as can be seen from the strong re-

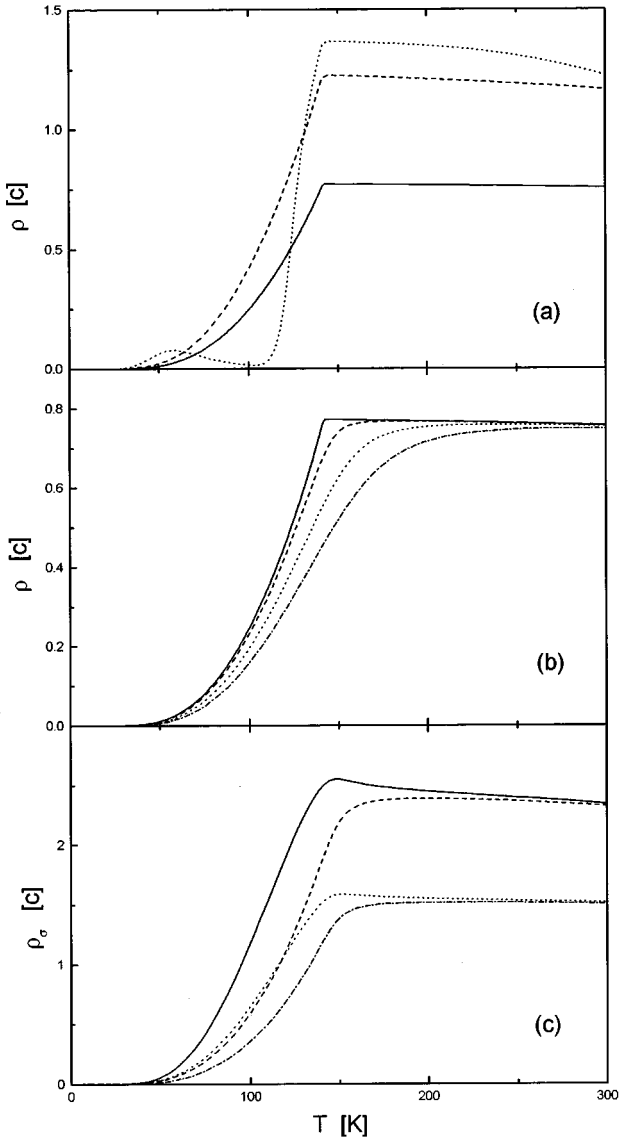

FIG. 4. Resistivity as a function of temperature. (a) Dependence on filling at $B=0$: $n=1.085$ (solid line), 0.15 (dashed line), and 1.055 (dotted line). (b) Dependence on magnetic field at $n=1.085$: $B=0$ (solid line), 1 T (dashed line), 4 T (dotted line), and 8 T (dot-dashed line). (c) Spin components of resistivity at $B=1$ T. At $n=0.15$, $\rho_\uparrow$ (solid line), and $\rho_\downarrow$ (dashed line); at $n=1.085$, $\rho_\uparrow$ (dot-dashed line), and $\rho_\downarrow$ (dotted line). Parameters as in Fig. 2. $c=(eV)^2/[n_c e^2 v_F^2 \hbar]$, e.g., $c\sim 0.1\ \Omega$ cm for $n_c\sim 10^{21}/\mathrm{cm}^3$ and $v_F\sim 10^7$ cm/s.

semblance of these curves to the experimental data around T_c.[7–10] An order of magnitude estimate for our resistivity results for $n=1.085$ is compatible with the values experimentally found [see Fig. 4(b)]. In any case the absolute value of resistivity we obtain depends on the total number of particles, as shown in Fig. 4(a).

Figure 4(c) shows the two components of the resistivity, one for each spin direction, at $B=1$ T and two fillings of Fig. 4(a). For a low total number of particles such that the Fermi level falls below the hybridization gap ($n=0.15$, here), the results can be qualitatively understood employing the impurity approximation. Here, at $T=0$ the spin-up resistivity is zero due to the absence of spin disorder, resulting in a null

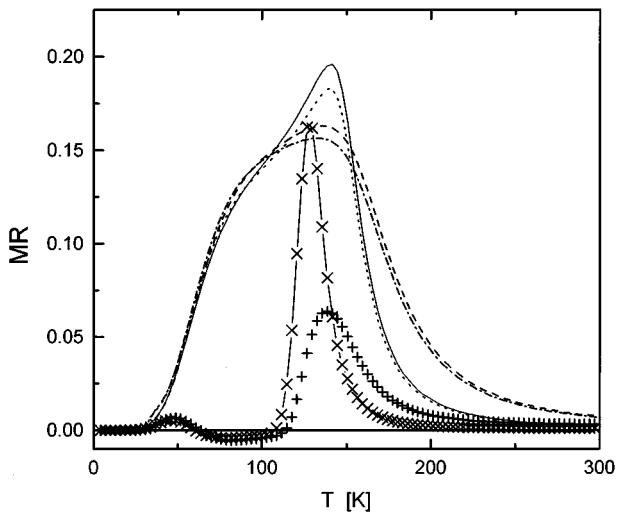

FIG. 5. Magnetoresistivity as a function of temperature. $\mathrm{MR}_{14}=[\rho_{1T}(T)-\rho_{4T}(T)]/\rho_{4T}(T)$, where $\rho_B(T)$ is the resistivity at temperature T and magnetic field B, for $n=1.085$ (solid line), 0.15 (dotted line), and 1.055 ($\times$). $\mathrm{MR}_{48}=[\rho_{4T}(T)-\rho_{8T}(T)]/\rho_{4T}(T)$ for $n=1.085$ (dashed line), 0.15 (dot-dashed line), and 1.055 (+). (MR data for $n=1.055$ plotted divided by 10.) Parameters as in Fig. 2.

self-energy. Also, the d-down density of states is zero [note the sum rule of Eq. (11)], and hence there is no spin-down resistivity at $T=0$. Increasing the temperature both resistivities build up along with spin disorder, dominating the spin-up one due to a higher d-up density of states at the Fermi level. Above T_c, one enters the paramagnetic phase and both resistivities tend to be very similar (equal for $B=0$). For a higher filling, e.g., the Fermi level slightly above the gap, like $n=1.085$, the spin components of resistivity appear inverted. Here hybridization gap effects on the CPA self-energy become relevant. At $T=0$, spin order again causes zero resistivity. But increasing temperature, the presence of the spin-up hybridization gap near the Fermi level produces an important increase in the real part of the CPA self-energy $\Sigma_{(d)\uparrow}$ for those energies. At temperatures below T_c, the absence of a hybridization gap in the spin-down density of states instead is reflected in a smoother behavior (and lower values) of the real part of the CPA self-energy $\Sigma_{(d)\downarrow}$. As a result of this the spin-up relaxation time (inversely proportional to the real part of the alluded CPA self-energy) and resistivity become smaller than their spin-down counterparts. This effect of split-band behavior on the real part of the CPA self-energy is well known from the general CPA theory.[26] For $n=0.15$, as the Fermi level falls in a region with an enhanced d-up density of states, a compensation of the effects of the real and imaginary parts of $\Sigma_{(d)\uparrow}$ on the relaxation time occurs, and the resistivity results can be explained in terms of the ''impurity approximation'' as done above. The absolute values of resistivity obtained for $n=1.085$ are lower than those for $n=0.15$, in accordance with general lower values of the d density of states. For cases of intermediate filling, with the Fermi level inside the gap, we find that the spin components of resistivity interpolate between the two regimes just described.

In Fig. 5 we plot the magnetoresistance results obtained,

employing the same parameters as above for the model. Here our results exhibit a difference in value between the magnetoresistivity maxima around T_c for lower (measured by MR_{14} here) and higher magnetic fields (given by MR_{48}) which is present in the experimental data.[9] We also reproduce the crossing of the magnetoresistivity curves for lower and higher magnetic fields which is found at temperatures above T_c. Our magnetoresistivity peak values for $n=1.085$ are approximately a factor 3 smaller than those which can be obtained from the data of Ref. 9. The features mentioned here as present in the experimental magnetoresistivity data were determined performing a scan of the resistivity curves of Ref. 9 and afterwards processing those data. Magnetoresistivity results obtained for fillings such that the Fermi level is placed inside either band, below and above the hybridization gap, are quite independent of the precise value of filling, which is not the case when the Fermi level falls inside the gap region. There, our results would indicate that higher values of magnetoresistance can be attained and shifts of MR peaks appear. In all, our description of the main features exhibited by transport measurements in $Tl_2Mn_2O_7$ around T_c is quite remarkable, considering the simplifications adopted in our treatment.

We will now refer to the implications for Hall transport experiments. In our case, two kinds of carriers are contributing to the transport, namely, conduction electrons of either spin direction. The ordinary Hall coefficient for the system, R_H, in terms of those for each type of carrier, R_σ ($\sigma=\uparrow,\downarrow$), takes the form[25]

$$R_H(\omega)=\frac{R_\uparrow\sigma_\uparrow^2+R_\downarrow\sigma_\downarrow^2}{\sigma^2}. \tag{17}$$

In the ferromagnetic phase, additional ''extraordinary'' or ''spin Hall'' terms in R_H, accounting for coupling between orbital motion of the carriers and the magnetization, may become important.[27]

The reports on Hall experiments for $Tl_2Mn_2O_7$ (Ref. 7) indicate the presence of electronlike carriers, about 0.001 conduction electrons per formula unit above T_c. In the ferromagnetic phase, the Hall coefficient is reported[7] to be field independent (for magnetic fields up to 6 T), no anomalous Hall signal is observed, and the number of carriers at low temperatures is about 3 times the value above T_c. We will interpret these facts on the basis of the results obtained with our model. The absence of anomalous Hall contributions below T_c would indicate that the ordinary Hall coefficient should suffice to explain the data. We shall assume a simple free-electron form for the Hall coefficient of each carrier species, namely, $R_\sigma=1/ecn_{c,\sigma}$, where $n_{c,\sigma}$ denotes the number of conduction electrons with spin σ contributing to transport. Consider the model with the parameters used above, and a filling such as $n=1.085$, i.e., the Fermi energy placed slightly above the gap in the density of states. At very low temperatures, the resistivities for spin up and spin down are both negligible. In such a case, from Eq. (17) the Hall coefficient would result: $R_H\sim(R_\uparrow+R_\downarrow)/4$. In the paramagnetic phase above T_c, again both conductivities tend to be similar, though being finite now, and the same formal expression for R_H holds. Nevertheless, the difference in R_H above and below T_c can be explained through the necessary change in $R_\downarrow$. With a gap (larger than k_BT) present in the density of states and the Fermi level lying (slightly) above the gap, it is only carriers in that upper (''conduction'') band which are effective for transport. This holds for spin-up electrons up to room temperature in our case, the resulting spin-up Hall coefficient having a negligible temperature dependence. For spin-down electrons, instead, there is no gap present in the ferromagnetic phase. Only at T_c has the spin-down c density of states developed a gap, similar to the spin-up one. Due to this fact, the number of spin-down electrons effective for transport is reduced above T_c, resulting in an increase of $R_\downarrow$ and R_H in accordance with experimental observations.[7,9]

Meanwhile, it is the total number of conduction electrons (which includes those below the gap and with our parameters is about 0.15, about 10 times the number of carriers above the gap) which would represent the real doping (x) into the Mn^{4+} state to take into consideration. In this way, the difficulties arising from the small number of carriers obtained from Hall data which are mentioned in Refs. 7 and 9 could be solved. It is interesting to note that a similar difficulty regarding the number of carriers detected and those doped into the sample had been mentioned by the authors of Ref. 28 when presenting their Hall data for TmSe.

To end this section, we now briefly comment on the transport results obtained with the impurity version of the model discussed above.[15] Using parameters for the impurity in accordance with those employed here for the periodic model and a filling such that the Fermi level falls slightly above the peak of the impurity density of states, we obtain magnetoresistance results very similar to those presented above. Nevertheless, the impurity picture would be hard to reconcile with the Hall data in $Tl_2Mn_2O_7$, indicating a very small number of carriers effective in transport.[7,9]

IV. SUMMARY

Summarizing, in this paper we have presented a complete discussion of the magnetotransport properties obtained with the intermediate-valence model model for the CMR pyrochlore compound $Tl_2Mn_2O_7$ which was proposed in Ref. 17. The model had been used before for the description of intermediate valence Tm compounds.[15,16] A lattice of intermediate-valence ions fluctuating between two magnetic configurations describes the Mn ions, which are hybridized with a conduction band which we relate to Tl. In this model, ferromagnetism originates from the IV lattice, but transport is intrinsically coupled to the magnetic configuration of the lattice (or spin disorder) through the scattering mechanism for conduction electrons which is determined by the hybridization. As a result of this coupling between magnetic order and transport properties, colossal magnetoresistance is obtained. We would like to observe that in spite of the simplifications adopted in our treatment of the model and the calculation of magnetotransport properties, the qualitative agreement between our results and the experimental data available on CMR pyrochlore $Tl_2Mn_2O_7$ is quite remarkable.

In connection with the model proposed here, it is important to mention that Shimakawa *et al.*[10] in a recent paper comment that the ferromagnetic metallic state and the magnetoresistance in pyrochlore $Tl_2Mn_2O_7$ are reminiscent of the

s-f interaction in europium chalcogenides and make a suggestion in favor of a mechanism for CMR similar to the one we propose[17] and our calculations substantiate. Europium chalcogenides have some features in common with mixed-valent Tm compounds, for which our model has been originally proposed.[15,16]

The presence of hybridization gaps or pseudogaps in the electronic structure, such as those considered here, could not only solve the problems posed by the Hall data which are mentioned by the authors of Refs. 7 and 9. They should cause observable effects in other experiments, such as spin-polarized tunneling and optical properties which are interesting to investigate. It is interesting to note that electronic structure calculations by Singh[14] for the ferromagnetic phase possess many features in common with our proposed band structure.

Concerning the strongly anisotropic approximation adopted here for the $S=1$ magnetic configuration, it should not introduce appreciable error for transport in the strongly ferromagnetic phase where spin-flip scattering processes are not allowed. The application of a magnetic field will also reduce spin-flip scattering processes, and so we would not expect major deviations from our magnetotransport predictions by relaxing this approximation. In any case, in the framework of the model and assuming $Tl_{2-x}^{3+}Tl_x^{2+}Mn_{2-x}^{4+}Mn_x^{5+}O_7$ the magnetization should be calculated considering $S=1$ and 3/2 magnetic configurations for the IV ions and deriving the magnetization from the free energy, though we do not expect major differences for magnetotransport results. A more accurate treatment of transport in presence of a hybridization gap in the density of states would be required to obtain better results for fillings such that the Fermi level lies in the gap region. Also, a realistic calculation of the Hall coefficient for this material is a nontrivial and interesting problem.

ACKNOWLEDGMENT

The authors are members of the Carrera del Investigador Científico of CONICET (Consejo Nacional de Investigaciones Científicas y Técnicas, Argentina).

[1] G. H. Jonker and J. H. Van Santen, Physica (Utrecht) **16**, 337 (1950).
[2] C. Zener, Phys. Rev. **82**, 403 (1951); P. W. Anderson and H. Hasegawa, *ibid.* **100**, 675 (1955); P. G. de Gennes, *ibid.* **181**, 141 (1960).
[3] R. Von Helmholt, J. Wecker, B. Holzapfel, L. Schultz, and K. Samwer, Phys. Rev. Lett. **71**, 2331 (1993); S. Jin *et al.*, Science **264**, 413 (1994).
[4] R. Allub and B. Alascio, Solid State Commun. **99**, 613 (1996); R. Allub and B. Alascio, Phys. Rev. B **55**, 14 113 (1997); Q. Li, J. Zang, A. R. Bishop, and C. M. Soukoulis, *ibid.* **56**, 4541 (1997).
[5] A. J. Millis, P. B. Littlewood, and B. I. Shraiman, Phys. Rev. Lett. **74**, 5144 (1995); A. J. Millis, B. I. Shraiman, and R. Mueller, *ibid.* **77**, 175 (1996).
[6] S. Yunoki, J. Hu, A. L. Malvezzi, A. Moreo, N. Furukawa, and E. Dagotto, (unpublished).
[7] Y. Shimakawa, Y. Kubo, and T. Manako, Nature (London) **379**, 55 (1996).
[8] S. W. Cheong, H. Y. Hwang, B. Batlogg, and L. W. Rupp, Jr., Solid State Commun. **98**, 163 (1996).
[9] M. A. Subramanian, B. H. Toby, A. P. Ramirez, W. J. Marshall, A. W. Sleight, and G. H. Kwei, Science **273**, 81 (1996).
[10] Y. Shimakawa, Y. Kubo, T. Manako, Y. Sushko, D. Argyriou, and J. D. Jorgensen, Phys. Rev. B **55**, 6399 (1997).
[11] H. Fujinaka, N. Kinomura, and M. Korizumi, Mater. Res. Bull. **14**, 1133 (1979).
[12] N. P. Raju, J. E. Greedan, and M. A. Subramanian, Phys. Rev. B **49**, 1086 (1994).
[13] D. K. Seo, M. H. Whangbo, and M. A. Subramanian, Solid State Commun. **101**, 417 (1997).
[14] D. J. Singh, Phys. Rev. B **55**, 313 (1997).
[15] C. A. Balseiro, and B. Alascio, Phys. Rev. B **26**, 2615 (1982); J. Mazzaferro, C. A. Balseiro, and B. Alascio, Phys. Rev. Lett. **47**, 274 (1981).
[16] J. Mazzaferro, Ph.D. thesis, Instituto Balseiro, Universidad Nacional de Cuyo, 1982; A. A. Aligia, J. Mazzaferro, C. A. Balseiro, and B. Alascio, J. Magn. Magn. Mater. **40**, 61 (1983); A. A. Aligia, Ph.D. thesis, Instituto Balseiro, Universidad Nacional de Cuyo, 1984.
[17] C. I. Ventura and B. Alascio, Proceeds. cond-mat/9702127 (unpublished).
[18] J. Fontcuberta *et al.*, Phys. Rev. Lett. **76**, 1122 (1996).
[19] P. Soven, Phys. Rev. **156**, 809 (1967).
[20] J. Mazzaferro, C. A. Balseiro, and B. Alascio, J. Phys. Chem. Solids **46**, 1339 (1985).
[21] O. Sakai, S. Seki, and M. Tachiki, J. Phys. Soc. Jpn. **45**, 1465 (1978).
[22] Y. Lassailly, A. K. Bhattacharjee, and B. Coqblin, Phys. Rev. B **31**, 7424 (1985).
[23] B. Velický, Phys. Rev. **184**, 614 (1969).
[24] F. Brouers and A. V. Vedyayev, Phys. Rev. B **5**, 348 (1972); F. Brouers, A. D. Vedyayev, and M. Giorgino, *ibid.* **7**, 380 (1973).
[25] R. E. Peierls, *Quantum Theory of Solids* (Clarendon Press, Oxford, 1955).
[26] B. Velický, S. Kirkpatrick, and H. Ehrenreich, Phys. Rev. **175**, 747 (1968).
[27] S. Legvold, in *Magnetic Properties of Rare Earth Metals*, edited by R. J. Elliott (Plenum, New York, 1972), p. 376.
[28] P. Haen, F. Lapierre, J. M. Mignot, and R. Tournier, J. Magn. Magn. Mater. **15-18**, 989 (1980).